Research Report 2016-02

Prediction of the sub-seasonal tropical cyclone genesis in the South Pacific: (I) Predictor identification

Ok-Yeon Kim

APCC
APEC CLIMATE CENTER

Research Report 2016-02

Prediction of the sub-seasonal tropical cyclone genesis in the South Pacific: (I) Predictor identification

Ok-Yeon Kim

APCC
APEC CLIMATE CENTER

PREFACE

Skillful predictions of subseasonal to seasonal tropical cyclone (TC) activities are important in mitigating potential destruction from the tropical cyclone approach and landfall in many South Pacific coastal regions. With the improvement in subseasonal to seasonal climate forecasts, more attention has been given to the details of subseasonal to seasonal tropical cyclone activity.

The objective of this study is to establish a week-long tropical cyclone activity prediction system in zones of the South Pacific during forthcoming weeks. The three key activities to accomplish this research goal are as follows: 1) investigation of physically meaningful weekly tropical cyclone variability, which is predictable; 2) identification of potential predictors associated with weekly tropical cyclone variability from physical consideration; and 3) development of the forecast model with selected predictors and examination of the model's performance in predicting subseasonal tropical cyclone activity. This study is designed as a three-year project: 1) Year 1: identification of potential predictors for subseasonal tropical cyclone genesis; 2) Year 2: development and verification of prediction model for subseasonal tropical cyclone genesis prediction; and 3) Year 3: improvement of the prediction model and visualization (including outreach). This year, we focused on the identification of possible sources (i.e., potential predictors) associated with weekly tropical cyclone variability from physical consideration.

Based on the composite analysis, the Madden-Julian Oscillation (MJO) phase has a strong relationship with subseasonal tropical cyclone genesis in the South Pacific Ocean. The THORPEX Interactive Grande Global Ensemble (TIGGE) forecasts are capable of predicting the MJO itself. Therefore, it would be reasonable to use the MJO forecasts from TIGGE as one of the primary predictors for weekly tropical cyclone genesis prediction. Given the collocation of the large cyclonic vorticity and tropical cyclone genesis areas, it is reasonable to use the relative vorticity averaged in each zone, instead of directly using various characteristics from the South Pacific Convergence Zone (SPCZ). Based on the relationship between the climatological seasonal cyclone of tropical cyclone activity and the local relative vorticity, the area-averaged relative vorticity field is regarded as a good predictor for weekly tropical cyclone genesis prediction, especially for regions West of the dateline. Considering the relationship between ensemble (ENS) and weekly tropical cyclone genesis probabilities for each zone, we decided to use the Nino3.4 index calculated from TIGGE forecasts as one of the predictors for the weekly TC genesis prediction.

There is room for further improvement of subseasonal tropical cyclone forecasts. In the coming successive research, we will focus on improving potential predictors by including a multi-model grand ensemble approach to forecast MJO and considering other physical and dynamical variables in addition to MJO, SPCZ, and ENSO. We will also focus on the statistical modeling issue to develop a reliable subseasonal tropical cyclone forecast model and conduct a stepwise predictor screening in the following research efforts on this topic.

Indeed, the successful completion of this study was made possible by the dedication of the researchers in APCC and academia involved in conducting the studies. I would like to express my special gratitude to research fellow Dr. Ok-Yeon Kim for her hard work and dedication in successfully managing and completing this project.

Dr. **Hong-Sang Jung**
President, APEC Climate Center
January 2017

ABSTRACT

The objective of this study is to establish a system for predicting the tropical cycle (TC) activity in the South Pacific zones during week-long periods. There are three key requirements to accomplish this objective. First, an investigation of physically meaningful and predictable weekly TC variability is required. Second, based on physical considerations, potential predictors associated with weekly TC variability need to be identified. Third, a forecast model based on selected predictors needs to be developed and model performance in predicting sub-seasonal TC activity evaluated. This study is designed as a three-year project. Year 1 (2016): identification of potential predictors for sub-seasonal tropical cyclone genesis. Year 2 (2017): development and verification of a model for predicting sub-seasonal tropical cyclone genesis. Year 3 (2018): improve the prediction model and disseminate the results, including outreach. In this report, we will focus on the identification of possible sources (i.e., potential predictors) associated with weekly TC variability based on physical considerations.

Based on composite analysis, the MJO phase has a strong relationship with sub-seasonal TC genesis in the South Pacific Ocean. TIGGE forecasts are capable of predicting the MJO itself; therefore, it is reasonable to use MJO forecasts from TIGGE as one of the primary predictors of weekly TC genesis prediction. Various SPCZ characteristics, strength, area, centroid latitude/longitude, are dominated by either seasonal or semi-annual variability. However, the maximum relative vorticity axis always lies 6°–10°S to the south of the SPCZ position, independent of its wide year-to-year excursions. Given the collocation between the large cyclonic vorticity

and TC genesis areas, it is reasonable to use relative vorticity averaged in each zone instead of directly using various SPCZ characteristics. Based on the relationship between the seasonal climate cycle of TC activity and local relative vorticity, the area-averaged relative vorticity field is regarded as a good predictor for weekly TC genesis prediction, especially for regions west of the dateline. Considering the relationship between ENSO and weekly TC genesis probabilities for each zone, we decided to use the Nino3.4 index calculated from TIGGE forecasts as one predictor of weekly TC genesis. Based on the relationship between the seasonal cycle of TC activity and ENSO phases, TC genesis increased east of the dateline in the warm phase ENSO years, and increased in the western part in the cold phase ENSO years.

There is a room for further improvement of potential predictors. For instance, the terms used to generate the Genesis Potential (GP) index will be further considered. The four different terms in GP index are absolute vorticity at 850 hPa, relative humidity at 700 hPa, vertical wind shear between 850 and 200 hPa, and maximum potential intensity. As the GP index empirically quantifies the effects of large-scale environment on tropical cyclogenesis, and considers both thermodynamic and dynamic factors for cyclogenesis, the consideration of terms in GP index would be good predictors for sub-seasonal TC genesis prediction. This work will be done in the next year.

Even though all predictors can explain part of the sub-seasonal TC activity, the inclusion of as many potential predictors as possible in the multivariate regression does not necessarily guarantee better predictability. In particular, for the case of mutually correlated potential predictors with stepwise procedures for determining the predictor, screening is required in the logistic regression. We will use the stepwise regression approach to select a best set of predictor variables from pools of potential predictors for each zone and each forecast lead-time. This work will also be done in the next year.

CONTENTS

1. INTRODUCTION ---------- 1

1.1 Background and motivation ---------- 1

1.2 Research objectives ---------- 3

2. DATA ---------- 5

2.1 TC best track dataset ---------- 5

2.2 TIGGE forecast ---------- 5

2.3 Reanalysis data ---------- 7

3. CLIMATOLOGY OF TC GENESIS IN THE SPO AND THE ASSOCIATED BASIC STATE ---------- 8

4. TARGET ZONE OF INTERESTS ---------- 11

5. SEASONAL CYCLE OF WEEKLY TC PROBABILITIES 12

6. IDENTIFICATION OF POTENTIAL PREDICTORS ---------- 15

6.1 MJO ---------- 15

6.1.1 Relationship between MJO phase and TC genesis ---------- 15

6.1.2 MJO predictability with TIGGE ---------- 17

6.2 SPCZ ---------- 22

6.2.1 SPCZ variability and relationship with TC genesis ---------- 22

6.3 ENSO ---------- 26

6.3.1 Relationship between ENSO and TC genesis ---------- 26

7. SUMMARY ---------- 28

8. FUTURE PLANS ---------- 30

8.1 Improvement of predictors ---------- 30

8.2 TC statistical forecast model ---------- 31

8.3 Statistical modeling issues ---------- 31

8.4 Stepwise predictor screening ---------- 32

REFERENCE ---------- 34

1. INTRODUCTION

1.1 Background and motivation

Accurate predictions of tropical cyclones (TCs) activity can benefit emergency preparedness and disaster mitigation in many coastal regions in the South Pacific. As short lead-time forecasts, high-resolution numerical weather prediction models can provide accurate forecasts of the genesis and tracks of individual TCs out to approximately five days (WMO 2016). However, beyond this time scale, the nature of the atmosphere makes it impossible to forecast individual TCs, and instead TC activity statistics, such as their genesis or frequency, are predicted. With the improvement in seasonal climate prediction, more attention has been given to successful seasonal TC activity forecasts in various basins (e.g., Vitart 2006; Camargo and Barnston 2009; Alessandri et al. 2011; Goh and Chan 2010, 2012; Kim and Webster 2010). However, relatively little effort has been given to the prediction of TC activity on sub-seasonal time scales. Motivated by this framework, the ultimate aim of this research is to provide reliable probabilistic information on TC occurrence in the South Pacific during week-long periods.

The tropical outlook is an official product of the National Oceanic and Atmospheric Administration (NOAA) Climate Prediction Center (CPC), which includes regions where tropical cyclogenesis is favored for the upcoming week-1 and week-2 time periods (http://www.cpc.ncep.noaa.gov/products/precip/CWlink/ghazards/index.php). Tropical cyclone areas from the outlook are subjectively created based on various objective forecast tools, such as Madden-Julian oscillation (MJO) composites, statistical and dynamical tropical cyclone forecasts, and raw model forecast guidance. Paul Roundy forecasts (http://www.atmos.albany.edu/facstaff/roundy/tcforecast/tcforecast.html) experimentally provide probability TC forecasts and anomalies, which are based on seasonal and 100-day low-pass patterns and/or MJO patterns. The European Centre for Medium-range Weather Forecasts (ECMWF) employs 32-day Ensemble Prediction System (EPS) for weekly mean tropical cyclone strike probability. Leroy and Wheeler (2008) also developed a purely statistical prediction system with several predictors based on seasonal tropical cyclone activity in the South Pacific. Even though both statistical and dynamical methods are capable of predicting sub-seasonal

TC activity during several weeks, the hybrid dynamical-statistical model potentially improves accuracy for sub-seasonal TC activity forecasts beyond that of component models. In a hybrid dynamical-statistical model, dynamic model-based predictions of large-scale variables can be used as a set of predictors for forecasting the statistical TC activity (e.g., occurrence) during several upcoming weeks. Therefore, the ultimate aims of this study are to provide reliable probabilistic information on sub-seasonal TC occurrence forecasts in the South Pacific through a hybrid dynamical-statistical model.

For a successful sub-seasonal TC activity forecast, it is important that we identify possible indicators of sub-seasonal predictability for South Pacific tropical cyclones and demonstrate model capabilities. Sub-seasonal variations in tropical convective activity play a significant role in the coupled atmosphere-ocean system and MJO is the strongest mode of tropical sub-seasonal atmospheric variability (Madden and Julian 1994). Many previous studies have demonstrated both an extended-range predictability of MJO out to about 20 days (e.g., Waliser et al. 1999; Lo and Hendon 2000), and the existence of strong contemporaneous relationship between MJO and TC activity (e.g., Maloney and Hartmann 2000; Hall et al. 2001). In combination, these two pieces of evidence support using MJO as one of the potential predictors of weekly TC activity, which is outlined in this work.

Several statistical models have been developed for MJO predictions based on various statistical methods, such as a regression using an empirical orthogonal function (EOF; Jones et al. 2004; Jiang et al. 2008), singular spectrum analysis (Mo 2001), and wavelet analysis (Webster and Hoyos 2004). Kand and Kim (2010) compared the performance of these statistical models in simulating MJO and indicated that the multi-regression method shows the best skill. Jiang et al. (2008) and Jones et al. (2004) demonstrated that the multi-regression model has an MJO predictability with the time scale of a few weeks. Dynamical models are applicable to MJO forecasts, which have some usefulness in predicting the MJO for some seasons compared to statistical models (e.g., Seo et al. 2009; Kang and Kim 2010; Matsueda and Endo 2011; Lin et al. 2008; Gottschalck et al. 2010). In particular, Matsueda and Endo (2011) demonstrated that operational medium-range ensemble forecasts, available at THe Observing system Research and Predictability Experiment (THORPEX)

Interactive Grand Global Ensemble (TIGGE) data portal, perform well in simulating the maintenance and onset of MJO in some phases.

In addition to MJO, there are other possible indicators of sub-seasonal prediction of South Pacific TC activity. The physical basis for TC activity prediction depends on information indicating that the large-scale environment favors TC genesis. Frank (1987) documented the necessary conditions for TC genesis: warm local sea surface temperatures coupled with a relatively deep oceanic mixed layer, large cyclonic absolute vorticity in the lower troposphere, weak vertical wind shear over the pre-storm disturbance, and high mid-level humidity. The key to TC activity prediction is identifying physically meaningful and predictable phenomena that affect conditions related to TC activity. Therefore, we consider likely and/or possible potential predictors in addition to MJO for weekly TC activity predictions. Possible predictors include SST variability in the Indo-Pacific associated with ENSO, interannual variability associated with SST (local SST) (Leroy and Wheeler 2008), and low-level relative vorticity anomalies (Hall et al. 2001). Vincent et al. (2009) also studied the location of the South Pacific Convergence Zone (SPCZ) as a strong modulator of atmospheric circulation variability in the South Pacific, and accordingly generating TCs. With careful investigation and selection of the aforementioned predictors, a prediction model was developed to predict the probability of TC occurrence in the South Pacific during upcoming weeks. Note that predictors used in real-time forecasting of TC occurrence in the hybrid model have to be uncorrelated, available in real-time, and without their own trend.

1.2 Research objectives

The objective of this study is to establish a system for predicting the TC activity prediction system in the South Pacific during week-long periods. Three key areas need to be addressed to accomplish this objective.

1) An investigation of physically meaningful and predictable weekly TC variability is required.

2) Based on physical considerations, potential predictors associated with weekly

TC variability need to be identified.

3) A forecast model based on selected predictors needs to be developed and model performance in predicting sub-seasonal TC activity evaluated.

A three-year plan for predicting sub-seasonal tropical cyclone genesis in the South Pacific is as follows:

- Year 1 (2016): identification of potential predictors for sub-seasonal tropical cyclone genesis.
- Year 2 (2017): development and verification of a model for predicting sub-seasonal tropical cyclone genesis.
- Year 3 (2018): improve the prediction model and disseminate the results, including outreach.

2. DATA

2.1 TC best track dataset

This study covers the austral summer season (NDJFMA; November-April) for the period beginning November 2006 to April 2015. The time period chosen for this study is consistent with the era over which the operational medium-range ensemble forecast system from TIGGE is available. The observational TC location data used in this study were obtained from the Joint Typhoon Warning Center (JTWC 2009) at 6 h intervals, available at https://metoc.ndbc.noaa.gov/JTWC/.

With the JTWC best track data, we consider all TCs in the tropical depression (TD) category (WMO 2014), formed in the South Pacific Ocean (SPO; 120°E-130°W in longitude and 0°S-40°S in latitude) during NDJFMA from 2006/2007 to 2014/2015. We use 92 storms in total based on this criteria. TC formation is defined as the first track point recorded in the JTWC database and is used interchangeably for genesis and occurrence throughout this study.

2.2 TIGGE forecast

The Observing system Research and Predictability Experiment (THORPEX) is a 10-year international research program organized by the World Meteorological Organization (WMO) with the purpose of improving the accuracy of one-day to two-week forecasts of severe weather events for societal, economical, and environmental benefit (WMO 2005). THORPEX have provided 10 global ensemble forecast datasets through TIGGE data portals (Bougeault et al. 2010) since October 2006. Using TIGGE is an effective mechanism for rapidly identifying severe weather events, such as tropical and extratropical cyclones, the MJO, and heavy rainfall and floods, and related phenomena (e.g., Froude 2010, 2011; Hamill 2012; Matsueda and Endo 2011; Matsueda and Nakazawa 2015). Table 1 summarizes the details of the ensemble prediction system (EPS). Although ensemble forecast data are available from several NWP centers (as in Table 1), the forecast data used in this study are obtained from operational medium-range ensemble forecasts from one of the leading global NWP centers, ECMWF.

The ensembles for outgoing longwave radiation (OLR) and 850 hPa and 200 hPa horizontal winds (U850 and U200) are obtained from the TIGGE portal at ECMWF (http://tigge.ecmwf.int) and are available with a two-day delay as part of the THORPEX research program for non-commercial research purposes only. The ECMWF ensemble forecast consists of 50 perturbation runs as well as one control run, and provides 15-day forecasts. This study analyzes the ensemble forecasts initialized at 00 UTC from November 1, 2006 to April 30, 2015. The forecast data are interpolated to a common grid spacing of 2.5° (latitude) by 2.5° (longitude).

Table 1 List of operational medium-range ensemble forecast system parameters (as of July 2016), available at the TIGGE portal: http://tigge.ecmwf.int/models.html. The nine operational medium-range ensemble forecast systems are based on their numerical weather prediction (NWP) centers: BOM (Bureau of Meteorology, Australia), CMA (China Meteorological Administration), CMC (Canadian Meteorological Center), CPTEC (Centro de Previsao de Tempo e Estudos Climaticos, Brazil), ECMWF (European Centre for Medium-range Weather Forecasts, UK), JMA (Japan Meteorological Agency), KMA (Korea Meteorological Administration), NCEP (National Centers for Environmental Prediction, USA), and UKMO (United Kingdom Meteorological Office)

NWP center	Forecast model resolution	Perturbation method	Perturbed area	Ensemble size/run	Maximum forecast length
BOM	TL119L19	SV[1]	90°-20°S, 20°-90°N	33	10days
CMA	TL213L31	BV[2]	Global	15	10days
CMC	0.9degL28	EnKF[3]	Global	21	16days
CPTEC	T126L28	EOF-based	45°S-30°N	15	15days
ECMWF	TL639L62 (0-10day) TL319L62 (10-15day)	SV[1]	90°-30°S, 30°-90°N + up to 6tropical areas	51 (1 control+50 perturbation)	15days
JMA	TL319L60	SV[1]	20°S-90°N	51	9days
KMA	T213L40	BV[2]	20°-90°N	17	10.5days
NCEP	T213L40	ETR[4]	Global	21	16days
UKMO	0.5555 (lat.) × 0.8333 (lon.) L70	ETKF[5]	Global	24	15days

[1] SV: Singular Vector, [2] BV: Bread Vector, [3] EnKF: Ensemble Kalman Filter, [4] ETR: Ensemble Transform with Rescaling, [5] ETKF: Ensemble Transform Kalman Filter

Several previous studies have investigated the predictability of TIGGE in terms of diverse atmospheric events. Su et al. (2014) evaluated TIGGE ensemble predictions for extreme summer precipitation. They showed that ECMWF generally performs best, while the CMC is relatively good for short-range (probabilistic) quantitative precipitation forecasts at light precipitation thresholds. Froude (2010, 2011) compared TIGGE predictions for extratropical cyclones using different ensemble prediction systems. In these studies, ECMWF ensemble mean and control have the highest level of skill for all cyclone properties (e.g., cycle position, intensity, and propagation speed). However, JMA, NCEP, UKMO, and CMC have one-day less skill for cyclone position throughout the forecast range. In addition, the relative performance of the different ensemble prediction systems remains broadly consistent between the two hemispheres.

2.3 Reanalysis data

OLR data produced by NOAA polar orbiting satellites are used. Wind field reanalysis datasets (U850 and U200) from the National Centers for Environmental Prediction-National Centers for Atmospheric Research (NCEP-NCAR) (Kalnay et al. 1996) are retrieved. Both datasets are obtained as daily means, interpolated onto a 2.5° (latitude) by 2.5° (longitude) common grid. The OLR, U200, and U850 datasets range from November 1980 to April 2004, and the multivariate EOF field is estimated for the basic MJO state. The OLR, U850, and U200 covering the period November 1, 2006 to April 30, 2015 are also used for calculating the observed MJO. Zonal and meridional winds (U850 and V850) from the NCEP-NCAR reanalysis covering November 1, 2006 to April 30, 2015 are retrieved to represent the low-level vorticity field. An annual cycle (mean plus first three annual harmonics) is calculated for each variable then subtracted from original values to produce daily anomaly fields.

3. CLIMATOLOGY OF TC GENESIS IN THE SPO AND THE ASSOCIATED BASIC STATE

Before discussing the modulation of TC genesis, it is relevant to understand the characteristic framework in which TCs and large-scale waves occur. It is also useful to know the seasonal and geographical distribution of the recorded TC formations in the target region. Figure 1 shows the monthly climate variation of TC occurrences from 1982/83 to 2013/14, which were calculated using TCs recorded in JTWC (as defined in Sec. 2.1). The number of TCs in each month indicates that most TCs occurred between November and April each year. In particular, January-March is the main period for TC occurrence in the South Pacific. TC occurrence is primarily concentrated west of the dateline (Figure 2), but TC occurs between 10°S-20°S throughout the SPO. Therefore, it is important to define the target zones of interest to develop weekly TC forecast models.

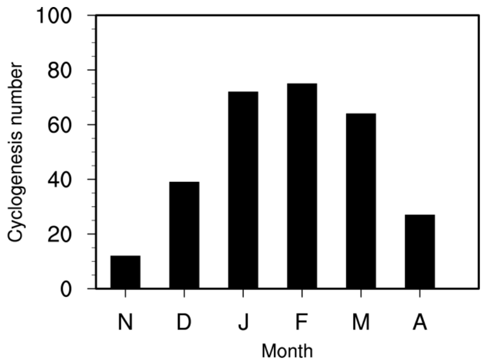

Figure 1 Monthly climate variation of TC occurrence in the SPO from 1982/83 to 2013/14 (32 years).

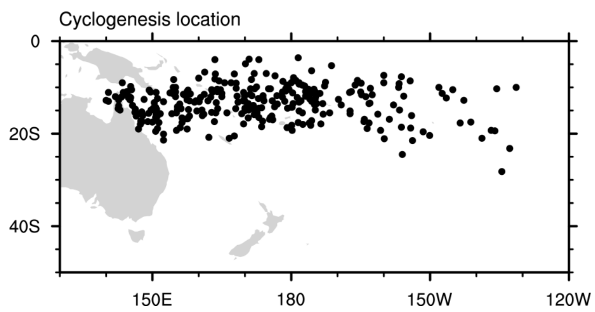

Figure 2 Geographical distribution of all TC genesis points in the SPO from 1982/83 to 2013/14 (32 years).

The formation and life cycle of TCs are associated with thermodynamic and dynamic conditions of the large-scale environment. Focusing on the dynamical aspects of the basic-state flow, the mean lower and upper-level wind fields for the austral summer (November-April) are displayed in Figures 3 and 4. At the upper level (Figure 3a), 200 hPa streamlines indicate the occurrence of westerlies poleward of 20°S, easterlies north of 10°S, and recurving flow in between. At the lower level (Figure 3b), 850 hPa streamlines show the anticyclone, centered on 30°S, 170°W. Cross-equatorial monsoon flow is present between the 0°-5°S latitudes, with the monsoon trough indicated by cyclonically recurving flow. Overall, Figures 3 indicates that the geographical position of TC genesis is located just poleward of the low-level monsoon trough and is collocated with the recurving flow in the upper level. Consistent with previous studies (e.g., Gray 1979; Dowdy et al. 2012; Hall et al. 2011), weak vertical wind shear and large cyclonic vorticity are favorable for TC genesis in the South Pacific Ocean.

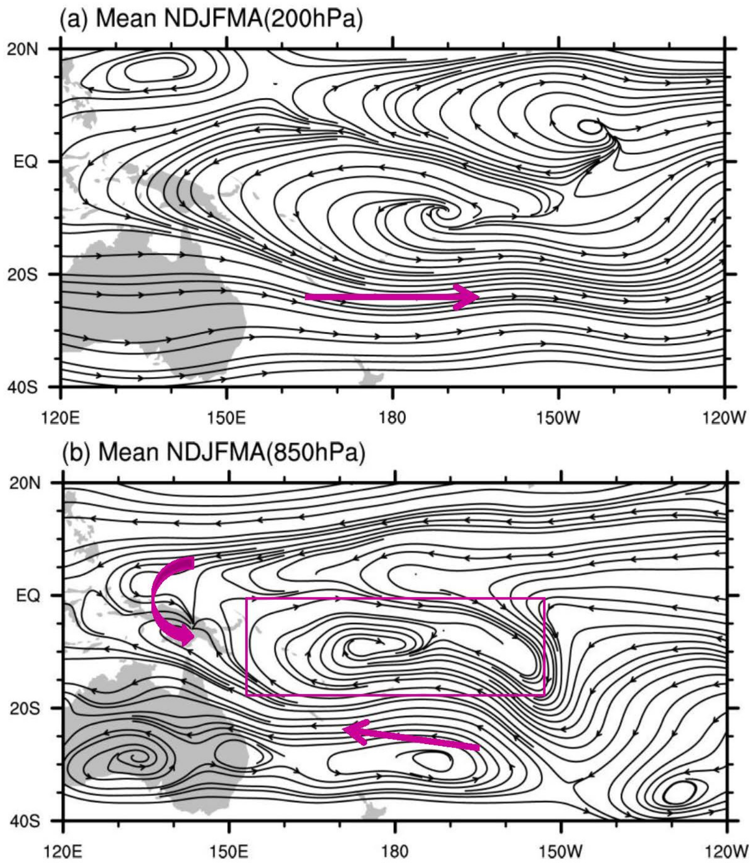

Figure 3 Austral summer (November-April) mean streamlines at the (a) 200 hPa and (b) 85- hPa levels.

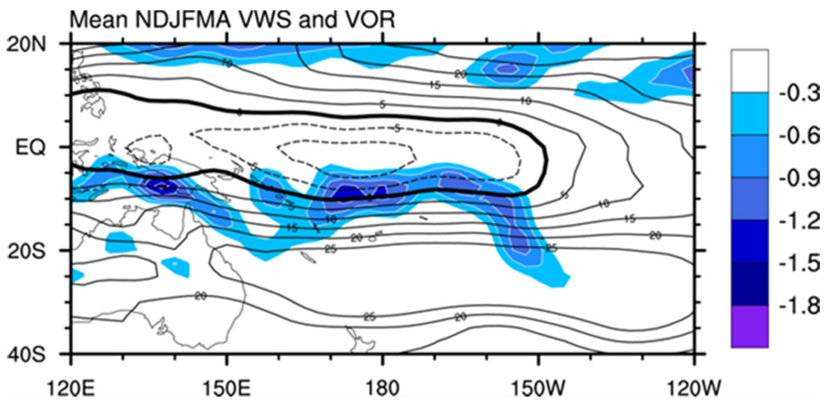

Figure 4 Austral summer (November-April) mean vertical shear of the zonal wind (contours) and 850 hPa vorticity (shading).

4. TARGET ZONE OF INTERESTS

The TC forecast model is developed in three different zones, as shown in Figure 5. The selection of these zones is based on physical consideration of TC activity in the SPO. The TCs that occur west of the boundary at 150°E have mean westward trajectories, whereas TCs that occur east of 150°E have mean eastward movement (Kim, 2015). The 180°E boundary (dateline) approximately separates regions that are well known to have contrasting responses to ENSO (Basher and Zheng 1995; Dowdy et al. 2012; Chand et al. 2013; Diamond et al. 2013). Latitudinal boundaries are set at 0°S to 30°S.

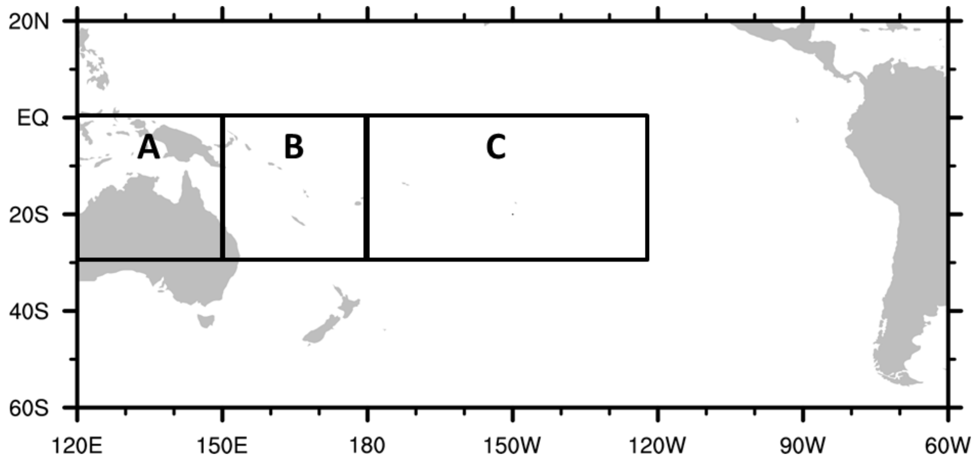

Figure 5 Several different zones; for each zone, a sub-seasonal TC occurrence prediction model was developed.

5. SEASONAL CYCLE OF WEEKLY TC PROBABILITIES

Figure 6 demonstrates seasonal climate cycle for weekly TC genesis probabilities (black histograms in Figure 6) from 2006 to 2015. Probabilities refer to TC genesis in the week starting on every day in a year. It is clear that the probability of TC genesis during a weak in January and February (i.e., the peak TC season) is much higher than in other months, indicating apparent seasonality of weekly TC probabilities. Due to the small sample size for averaging TCs, the raw climatological probabilities computed from daily data are noisy. Therefore, the raw probabilities are smoothed using Fourier analysis applied to the 365-day climate record reconstructed with the mean and first annual harmonics (red lines in Figure 6). The first harmonics account for about 40% of total variance and the second and higher harmonics have very small amplitudes compared to that of the first. As shown in Figure 6, the smoothed probabilities seem to more accurately reflect the real seasonal cycle of TC genesis. We use smoothed probabilities for seasonal climate cycles of weekly TC genesis hereafter.

To further verify the use of smoothing functions shown in Figure 6, the climatological monthly variation of TC occurrences from 1982/83 to 2013/14 is presented. The seasonal TC cycle for each region indicates that the first harmonic fitting functions are reasonable enough for weekly TC probability representations.

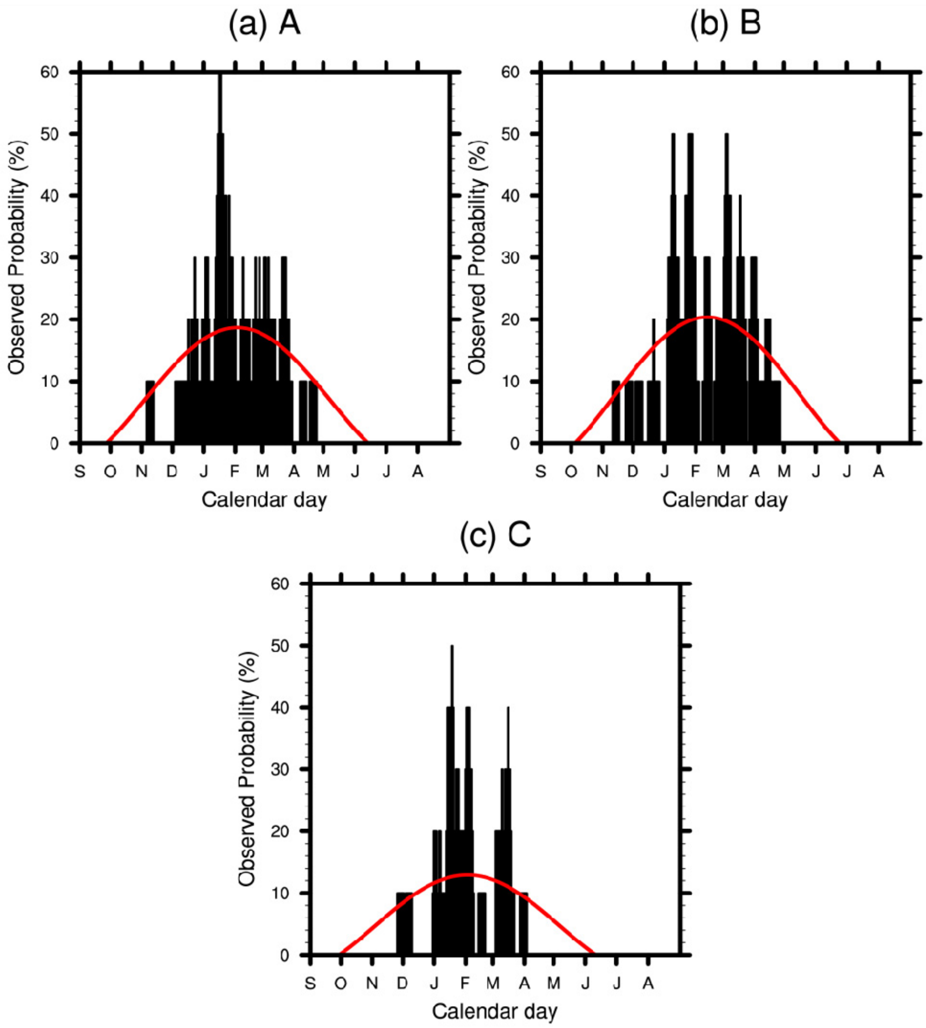

Figure 6 Seasonal climate cycles of weekly TC genesis probabilities for each zone shown in Figure 5. Probabilities (black histogram) refer to the probability of TC genesis in the week starting every day in during the active TC season from September to August. Red curves denote the weekly TC genesis cycle smoothed using Fourier analysis applied to the 365-day climatology and reconstructed using only the mean and the first annual harmonics.

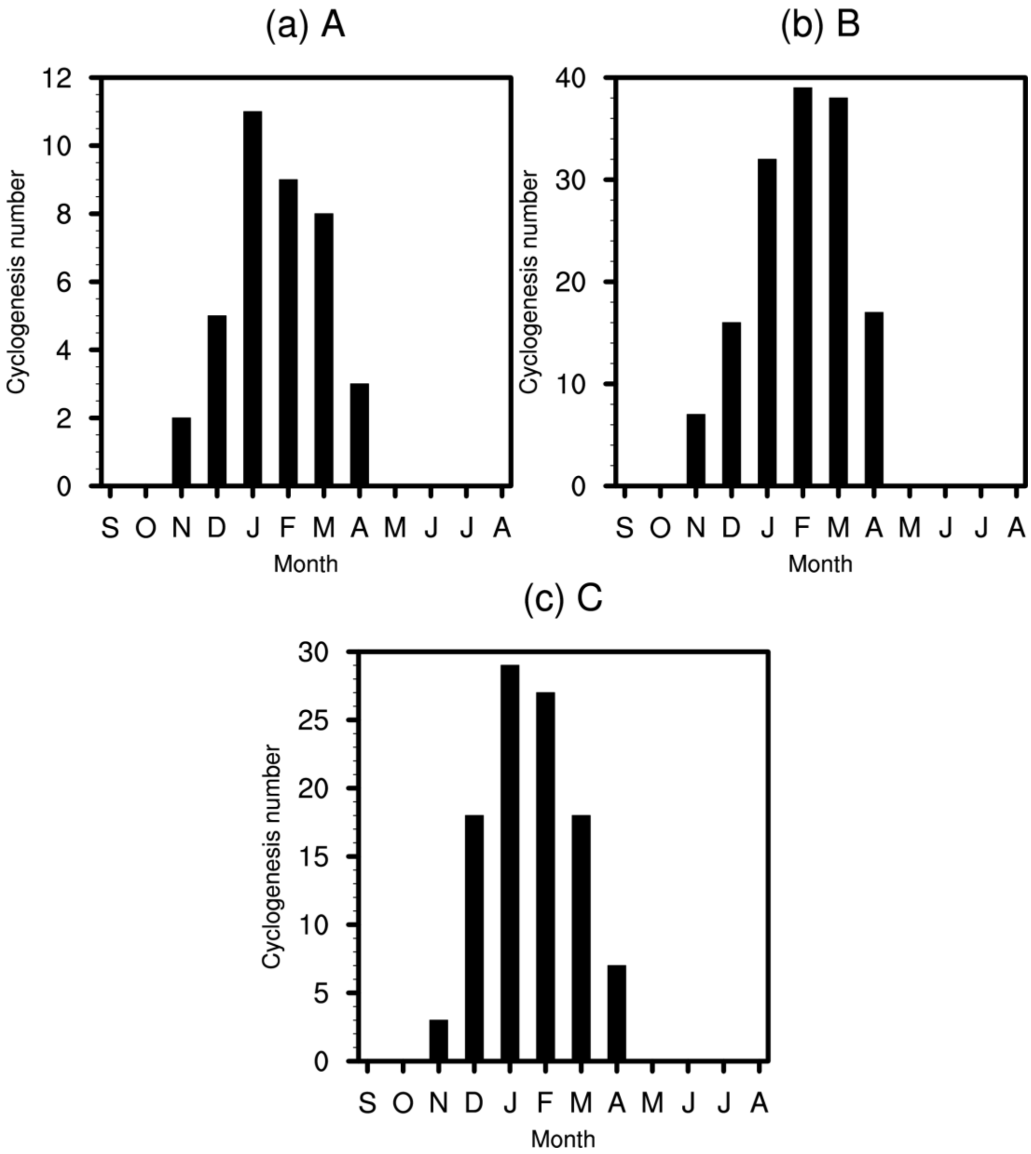

Figure 7 Monthly climate variation of TC occurrence in the SPO for each zone shown in Figure 5 from 1982/83 to 2013/14 (32 years).

6. IDENTIFICATION OF POTENTIAL PREDICTORS

6.1 MJO

6.1.1 Relationship between MJO phase and TC genesis

As mentioned in the introduction, the contemporaneous relationship between the RMM-based MJO phase and TC genesis in the South Pacific were well-established in several previous studies. Leroy and Wheeler (2008) binned TC genesis locations according to predefined MJO phase categories. They found that the TC genesis peaked in phase 4, 5, 6, and 7 near Australia, and 6, 7, 8, and 1 for South Pacific based on TC data for the years 1969-2004. Ramsay et al. (2012) conducted a cluster analysis of TC activity in the Southern Hemisphere and found that TC activity in the South Pacific is favored when the MJO-enhanced convection is located over the western Pacific and Western Hemisphere. More recently, Klotzbach (2014) hypothesized that TC genesis in the South Pacific is favored for MJO phases 6, 7, and 8, and unfavored for phases 1, 2, 3, and 4. Focusing on the FST (Fiji-Samoa-Tonga) region in the South Pacific, Chand and Walsh (2010) also recognized that TC occurrences increased in the active phase of the MJO, which is associated with enhanced convective activity in that region. All of these research studies indicated the potential for TC genesis and occurrence prediction with sub-seasonal lead time based on the MJO state.

The simultaneous relationship between the observed MJO index and TC genesis is demonstrated by binning the TC genesis locations for each MJO phase category (Figure 8). In Figure 8, the role of the MJO in modulating TC genesis can be recognized. Consistent with the results of previous studies (Hall et al. 2001; Frank and Roundy 2006; Leroy and Wheeler 2008), TC genesis locations tend to be located poleward and westward of the strong MJO convection. As discussed in Klotzbach (2014), TC genesis in northern Australia and the Coral Sea peaks in MJO phases 2, 3, 4, and 5 (Figure 8a, b). The peak of TC genesis in the South Pacific is during MJO phases 6, 7, 8, and 1, but TC genesis is less favored in MJO phases 2, 3, 4, and 5 (Figure 8c, d). In the case of weak MJO phases (Figure 8e), many TC genesis have also been found longitudinally near 10°S-20°S, implying other possible local factors that favor TC genesis.

Given the extended-range predictability of the MJO from TIGGE forecasts (in Sec. 2), and the existence of strong contemporaneous relationship between the MJO and TC occurrence, it is reasonable to use the MJO index calculated from TIGGE forecasts as two predictors for the TC forecast statistical model.

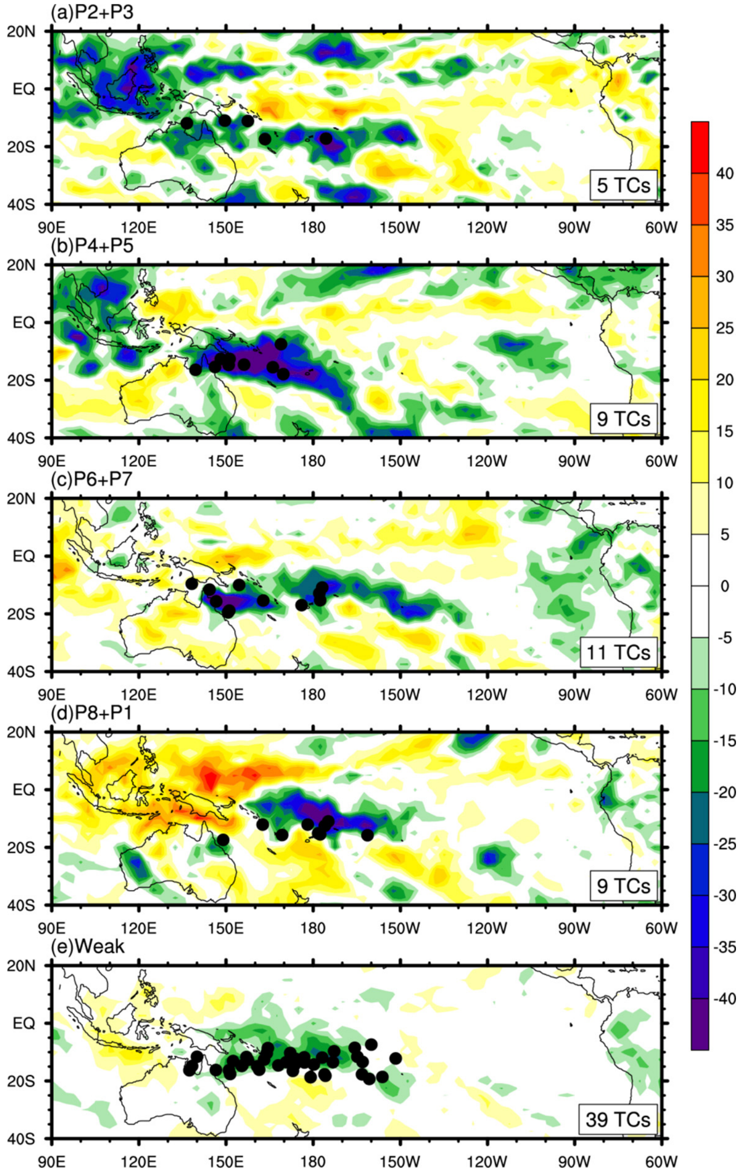

Figure 8 TC genesis locations (black dots) in each MJO phase, as defined by the RMM index. Also shown are OLR anomalies (shaded) for each averaged MJO phase. For simplicity, we combine two neighboring categories: (a) phases 2+3, (b) phases 4+5, (c) phases 6+7, and (d) phases 8+1. The bottom panel, (e) is the map for the weak MJO phases.

6.1.2 MJO predictability with TIGGE

Wheeler and Hendon (2004) proposed a real-time multivariate MJO index, for which OLR, U850, and U200 are used. The MJO index for the forecast is calculated by projecting combined forecast anomalies of 15°S-15°N meridionally averaged OLR, U850, and U200, normalized using observed standard deviations from NCEP/NCAR reanalysis, onto the two dominant EOFs (Figures 9 and 10) derived using the same meridionally averaged variables from the NCEP/NCAR reanalysis. Daily forecast anomalies are obtained by subtracting the first three harmonics of the annual cyclone from the forecast data and then removing the averages of the previous 120-days before projecting the observed EOFs. The annual cycle and 120-day averages are not available in the forecast data, and thus observed values are used. The MJO has nine different phases, in which phase 0 indicates the MJO is inactive; phases 1-4 are enhanced MJO phases with eastward propagation of a large-scale pattern of increased rainfall from the western Indian Ocean (phase 1) to the maritime continent (phase 4); and phases 5-8 are suppressed phases with decreased rainfall.

Figure 9 demonstrates the EOF spatial structures of the combined daily fields of the 15°S-15°N averaged OLR, U200, and U850 for NCEP/NCAR reanalysis from 1980 to 2004. The EOF shows the large-scale, eastward-propagating, convection-circulation patterns. Clearly, in the first EOF mode, the strong convective heat source is over the Maritime Continent and the western Pacific (100°E-160°E), whereas in the second EOF mode, there is strong convection over the Indian Ocean (60°E-100°E). The EOF patterns explain 12.0% and 11.6% of the total variability, respectively. It is also clear that the first EOF principal component (PC) time series leads the second EOF PC time series by a quarter of an MJO cycle, an approximately 10-12 day lag (Figure 10). This lead also corresponds to eastward movement of the convective anomalies over the warm pool region.

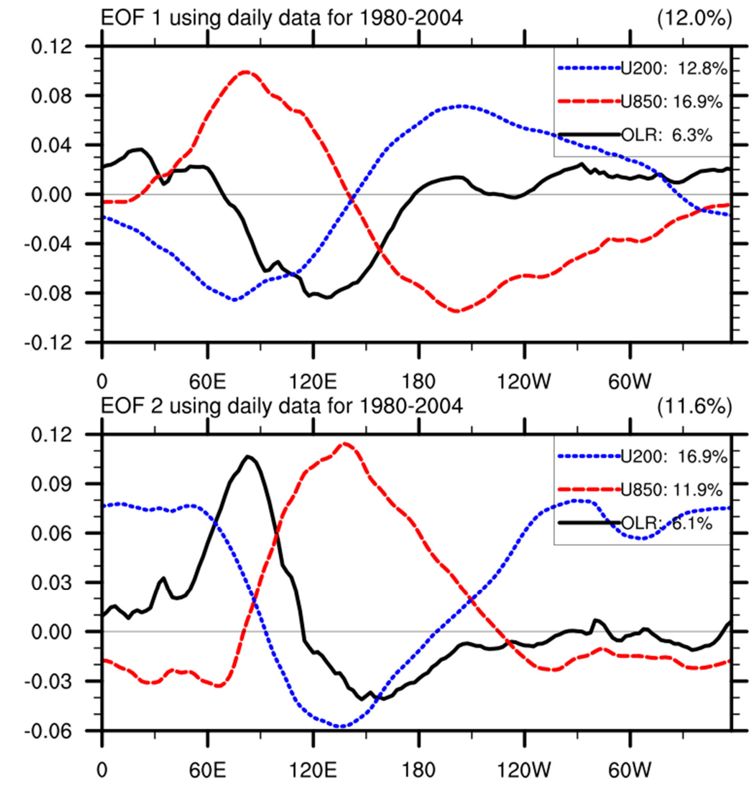

Figure 9 EOF1 (upper panel) and EOF2 (lower panel) of the combined daily field of the 15°S-15°N averaged OLR, U850, and U200. All variables are normalized using the averaged global variance value.

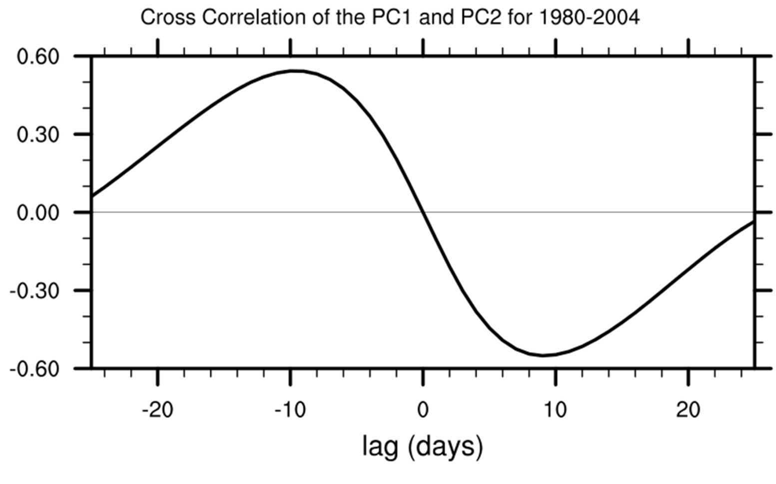

Figure 10 Cross correlation of the first EOF principal component (PC1) time series and the second time series (PC2) counterpart from 1980 to 2004.

We evaluate the performance of the MJO index forecast using the TIGGE/ECMWF forecast. Figure 11 shows a set of MJO forecast phase diagram examples from the ECMWF for 15 day outlooks, initialized once a day at 00 UTC from March 29, 2014 to 00 UTC on April 6, 2014. The MJO phase and amplitude forecasted from the ECMWF are in good agreement with those observed. In particular, the forecasted MJO phase and amplitude from the ensemble mean are well matched with those observed, showing good performance in predicting the MJO event. The MJO phase and amplitude at the initial forecast time correspond well with those observed, and this agreement is clear regardless of increasing forecast time.

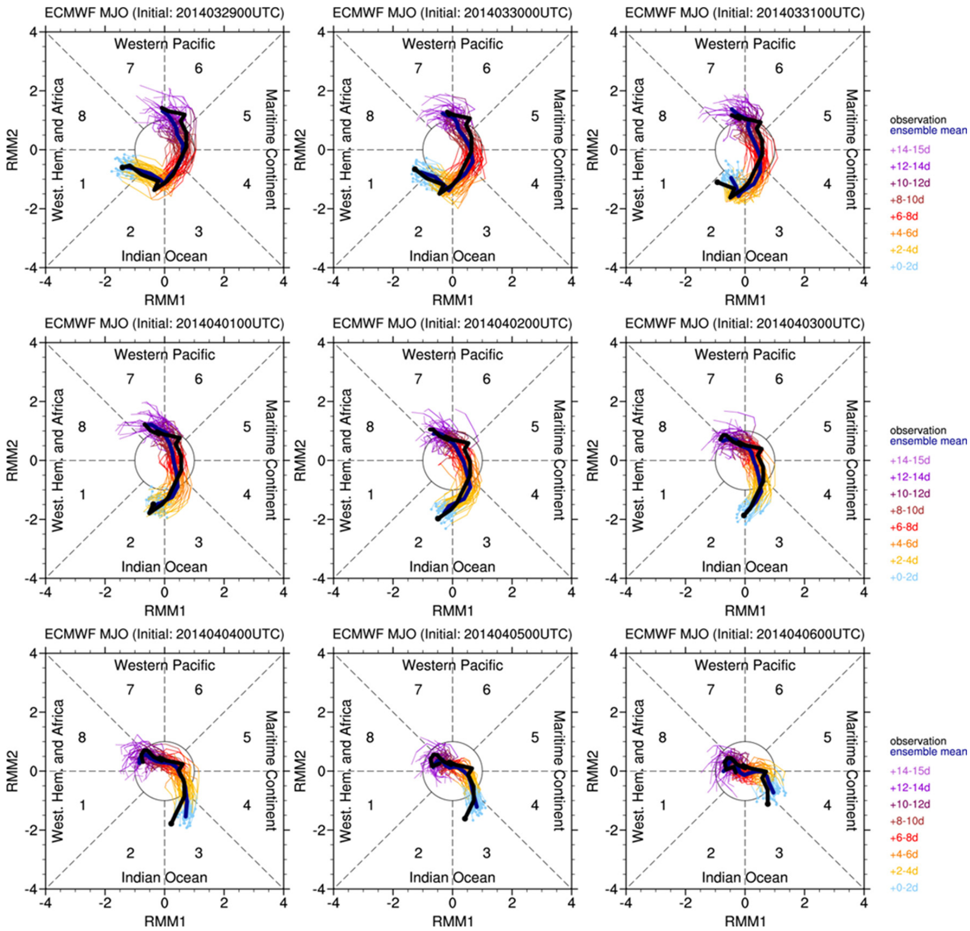

Figure 11 Snapshots of the MJO phase diagram for the real-time multivariate MJO index forecast using ECMWF from March, 29 to April 6, 2014. The black lines indicate observed RMM index, the blue lines indicate the ensemble mean forecasted RMM index from perturbed ECMWF ensemble runs. The other color lines indicate the forecasted RMM index from each perturbation ECMWF ensemble run.

Four standard verification scores for MJO forecasts are used in this study: root mean square error (RMSE), bivariate correlation (COR), phase error (PERR), and amplitude error (AERR). The definitions are respectively as follows:

$$RMSE^i(t,\tau)= \sqrt{\left(f_1^i(t,\tau)-a_1(t)\right)^2+\left(f_2^i(t,\tau)-a_2(t)\right)^2}$$

$$COR^i(t,\tau)= \frac{a_1(t)f_1^i(t,\tau)+a_2(t)f_2^i(t,\tau)}{\sqrt{a_1(t)^2+a_2(t)^2}\sqrt{f_1^i(t,\tau)^2+f_2^i(t,\tau)^2}}$$

$$PERR^i(t,\tau)= \tan^{-1}\left(\frac{a_1(t)f_2^i(t,\tau)-a_2(t)f_1^i(t,\tau)}{a_1(t)f_1^i(t,\tau)+a_2(t)f_2^i(t,\tau)}\right)$$

$$AERR^i(t,\tau)= \sqrt{f_1^i(t,\tau)^2+f_2^i(t,\tau)^2}-\sqrt{a_1(t)^2+a_2(t)^2}$$

where $f^i(t,\tau)=\left(f_1^i(t,\tau),f_2^i(t,\tau)\right)$ is the i-th ensemble member in each ensemble forecast in the MJO phase space, initialized at time $t-\tau$, and valid at time t; $a(t)=\left(a_1(t),a_2(t)\right)$ is the analyzed MJO index at time t. An RMSE of zero indicates a perfect MJO forecast in terms of both amplitude and phase, and a COR of zero indicates a perfect forecast regarding the MJO phase. PERR reveals the predicted phase speed relative to that observed, and AERR indicates the difference between the predicted and observed amplitude. These scores are calculated for each ensemble member at each lead time τ, and then each score is averaged over all ensemble members for the entire forecast period.

Figure 12 shows the MJO forecast skills as a function of forecast time, which is measured by the verification scores. ECMWF shows reasonable skill in terms of RMSE up to a lead time of nine days. After that, RMSE tends to increase but it is still small. In terms of CORR, ECMWF reveals good skill throughout the lead time, showing a CORR higher than 0.6. The phase speed (PERR) predicted by ECMWF is faster than that observed through the entire forecast lead time. In terms of amplitude error (AERR), ECMWF tends to have a smaller amplitude than that observed for most lead times, but AERR is very close to 0 through all lead times. In general, ECMWF shows reasonable skill regarding the MJO phase and amplitude. Comparing the MJO forecast from several TIGGE model sets, Matsueda and Endo (2011) demonstrated that ECMWF generally yields the best performances in predicting the MJO.

The performance of ECMWF in forecasting MJO activity is further examined. For each separate stage (i.e., developing, mature and decaying phases of MJO), PERR and AERR are compared. The developing (decaying) phase indicates MJO activity initialized at phase 0 (phase 1-8) and was verified at phases 1-8 (phase 0). The mature phase manifests an MJO activity initialized at phase 1-8 and verified at phase 1-8. From this, we obtain a more detailed forecast skill in terms of the MJO lifecycle. Figure 13 shows that ECMWF has better skill in terms of PERR and AERR for decaying MJO phases compared to other phases. However, for other phases (developing and mature), ECMWF still reveals reasonable skill in predicting MJO activity. PERR and AERR are very close to 0 regardless of MJO activity phase.

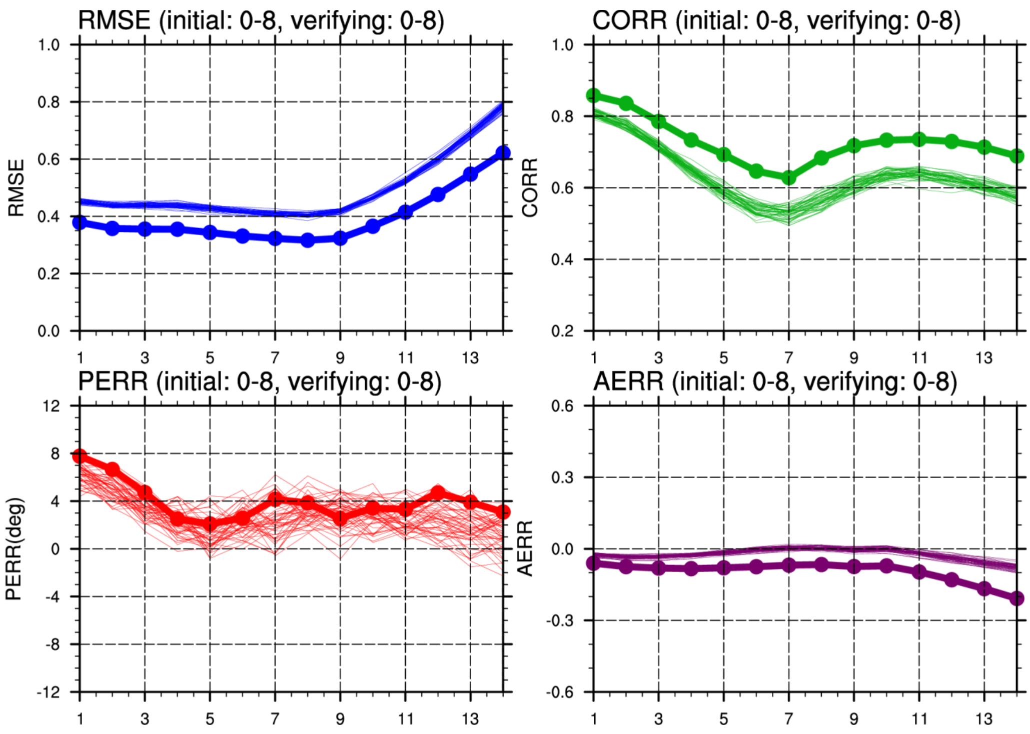

Figure 12 Root-mean square error (RMSE), bivariate correlation (CORR), phase error (PERR), and amplitude error (AERR) for real-time multivariate MJO index forecasts using ECMWF. The MJO forecasts skills are shown as a function of forecast lead time.

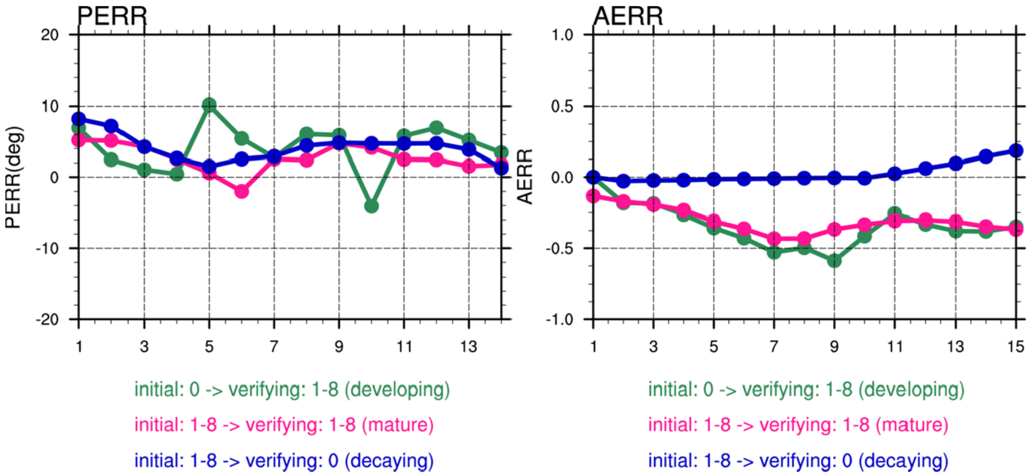

Figure 13 Phase error (PERR), and amplitude error (AERR) for real-time multivariate MJO index forecasts using ECMWF. The green (blue) lines indicate the developing (decaying) phase of MJO where the MJO is in phase 0 (phase 1-8) at day 0 and phases 1-8 (phase 0) at other days. The pink lines reveal mature phases of MJO where the MJO is in phase 1-8 at day 0 and phases 1-8 at other days.

6.2 SPCZ

6.2.1 SPCZ variability and relationship with TC genesis

The SPCZ is characterized by low-level convergence between the northeasterly winds west of the south Pacific high and cooler southeasterly winds from higher latitudes ahead of high pressure systems moving eastward from the Australia and New Zealand region (Barry and Chorley 2003). The SPCZ is more active in the austral summer and it is usually defined by the precipitation amount, as shown in Figure 14.

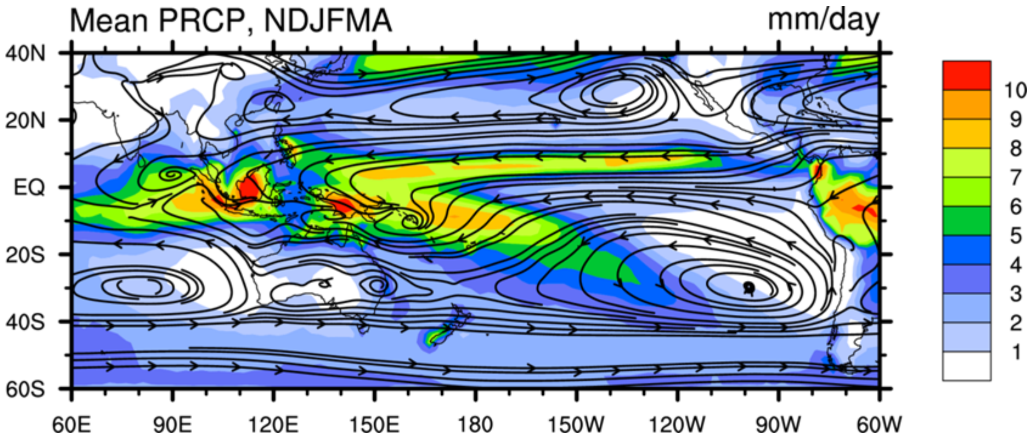

Figure 14 Climatology of November-April (active TC season in the SPO) precipitation (GPCP; Global Precipitation Climatology Project, version 2). Convergence zone positions are shown: Inter Tropical Convergence Zone (ITCZ) and South Pacific Convergence Zone (SPCZ). Dark black arrows are streamlines extracted from the NCEP-NCAR reanalysis NDJFMA-mean surface winds in the region.

The position of the SPCZ is considered a good indicator of cyclogenesis geography in the South Pacific because the SPCZ reveals large-scale dynamic and thermodynamic fields over the region (Vincent et al. 2009). Moreover, the small displacement in the mean SPCZ position can have a strong influence on the generation of TCs in the South Pacific. The SPCZ is characterized by a zonal portion located over the western Pacific warm pool region and a latitudinal tilt portion along the northwest-southeast axis. The interannual variability of its western portion is influenced by a monsoon trough that affects the Indian Ocean and Australian region, with monsoon winds extending eastward to the dateline (Vincent et al. 2009). However, the interannual variability of the eastern SPCZ relies on interactions with higher latitude depressions and on the existence of a dry zone in the southeastern Pacific (Kiladis et al. 1989; Widlansky et al. 2011). The daily to weekly scale variability of spatial location is controlled by zonal dry air inflow associated with trade wind strength (Lintner and Neelin 2008). The SPCZ strength, area and centroid latitude have a dominant seasonal cycle, whereas the SPCZ centroid longitude has a prominent intraseasonal variability due to MJO influence (Kidwell et al. 2015). Thus, the SPCZ variability is affected by various seasonal and/or intraseasonal phenomena.

TC genesis is known to be dependent on large scale dynamic and thermodynamic fields and surface cyclonic vorticity is one variable that favors TC genesis (Gray 1979). In particular, 850 hPa relative vorticity anomalies are an excellent diagnostic of changes in large-scale cyclogenesis patterns. (Hall et al. 2001; Vincent et al. 2011). Vincent et al. (2011) found that the SPCZ is always collocated with the zero relative vorticity at low levels. However, the maximum vorticity lies 6° to the south of the SPCZ position, which is independent of its interannual variation. They also demonstrated that this structure in the SPCZ region constrains tropical cyclogenesis to occur favorably within 10° south of the SPCZ location. This is consistent with other studies indicating that the location of the SPCZ controls cyclogenesis distribution, which occurs on the poleward side of the tropical portion of the SPCZ (Gray 1979; Vincent et al. 2011; Lorrey et al. 2012). Figure 15 depicts the composite 850 hPa relative vorticity for all TC genesis days in NDJFMA from 2006 to 2015. Consistent with previous studies, the TC genesis location is considerably collocated with the large relative cyclonic vorticity around 10°S-20°S, especially west of the dateline. Thus, cyclonic relative vorticity related to SPCZ can be a good indicator (i.e., predictor) for weekly TC genesis forecasts in the South Pacific.

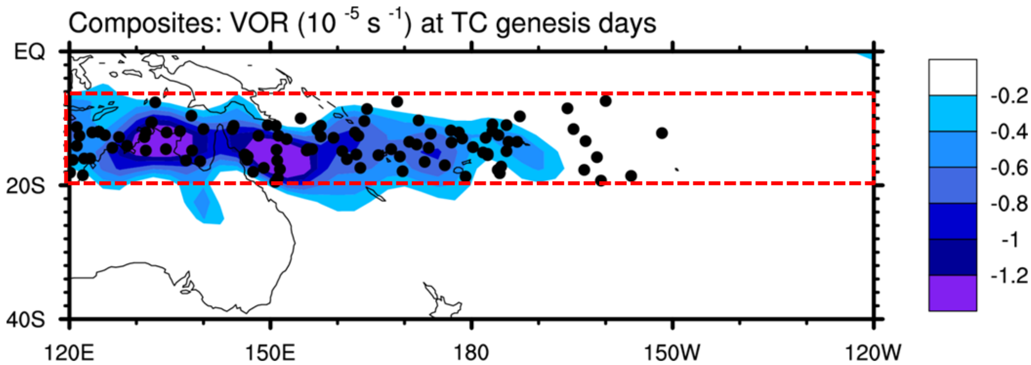

Figure 15 Shaded areas indicate mean cyclonic vorticity for all TC genesis days from 2006/11 to 2015/04. Black dots indicate the geographic locations of TC genesis.

The relationship between relative cyclonic vorticity and weekly TC genesis for each zone is further examined. Figure 16 demonstrates the seasonal cycle of relative vorticity peaks (averaged for 10°S-20°S for each zone) over a month when weekly TC genesis is the most active, especially for regions A and B (Figure 16a and b). However, the seasonal cycle of relative vorticity for region C peaks over a month earlier than that for TC genesis (Figure 16c). Thus the result in Figure 16 implies that the area-averaged relative vorticity field can be regarded as a good predictor for weekly TC genesis prediction for regions A and B, is not a good predictor for region C. Because the eastern position of the SPCZ (for region C) is tilted along the northwest-southeast direction, the zonally averaged relative vorticity would be insufficient to be used as a TC genesis predictor for that region. There are presumably other large-scale factors that affect TC genesis for the region (e.g., ENSO). Given the collocation between the large cyclonic vorticity and TC genesis areas in regions A and B (shown in Figure 15), we employ 850 hPa relative vorticity field averaged between 10°S-20°S in each zone, instead of directly using the SPCZ characteristic (e.g., area, position, and strength).

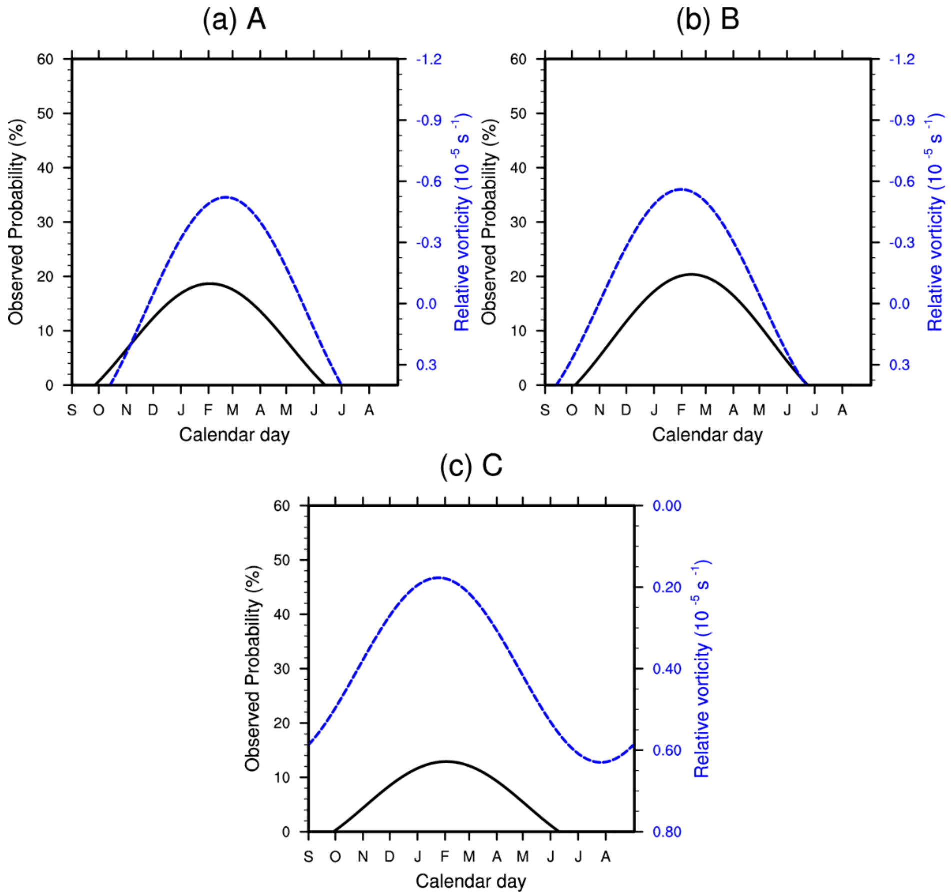

Figure 16 Seasonal climate cycle of TC activity (black curves) and local relative vorticity (blue curves) for each zone. Relative vorticity are averaged for the latitudes 10°S-20°S for each zone.

6.3 ENSO

6.3.1 Relationship between ENSO and TC genesis

It is well known that the key driver of TC genesis variability in the South Pacific is ENSO (e.g., Chand et al. 2013; Diamond et al. 2013; Dowdy et al. 2012). The authors have shown that the spatial patterns and characteristics of TC genesis in the South Pacific are related to the different phases of ENSO. In the positive ENSO phase, TC genesis is preferentially enhanced eastward to the South Pacific Ocean, with the highest TC density centered on the dateline. In the negative ENSO phase, TC genesis positions have their maximum density further west of the dateline, because equatorial convection moves further westwards.

Figure 17 represents the Nino3.4 index time series averaged for the TC active season (NDJFMA) from 2006/07 to 2014/15. From the time series, we select 2006/07, 2009/10, and 2014/15 as above-normal years, and 2007/08, 2010/11, and 2011/12 as below-normal years. We thus compare the simultaneous relationship between these two types of interannual SST variability and TC genesis for each zone. Figure 18 reveals that the TC genesis increases east of the dateline (region C) in the above-normal years (warm ENSO phase), consistent with previous studies. TC genesis in region A (far western of the dateline) indicates an increased TC probability in the below-normal years (cold phase of ENSO) during the TC peak season (January-February). This results is also consistent with the findings in previous studies. In region B, TC genesis probability tends to remain the same, regardless of the ENSO phase. This result implies that the Nino3.4 index, representing the behavior of ENSO, can be considered one potential predictor for weekly TC genesis forecasts.

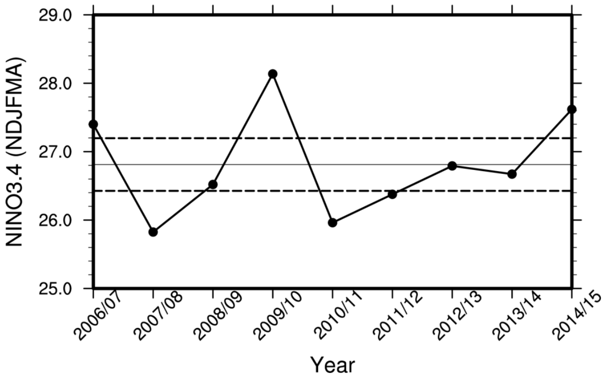

Figure 17 Time series of Nino3.4 index averaged for NDJFMA from 2006/07 to 2014/15. The gray solid line indicates the index mean during all periods, and the black dashed lines indicate the boundaries for 0.5 sigma of the index mean. From this, above-normal years are 2006/07, 2009/10, and 2014/15, and below-normal years are 2007/08, 2010/11, and 2011/12.

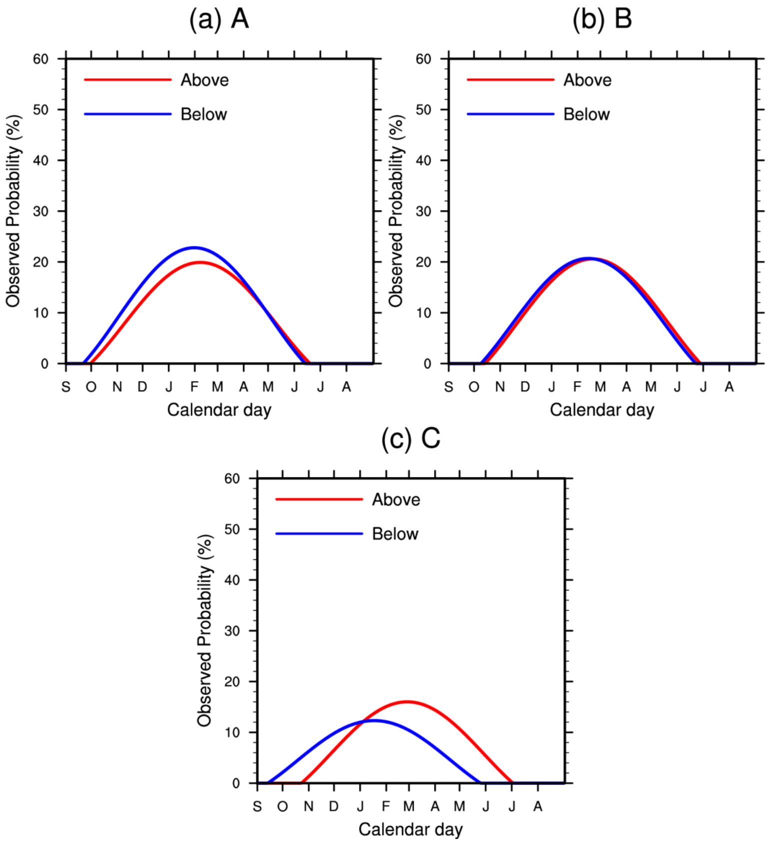

Figure 18 Seasonal climate cycle of TC activity for each zones. Above- (red) and below-normal (blue) years are defined in Figure 17. Note that above-and below-normal years correspond to warm- and cold-phase of ENSO years.

7. SUMMARY

This study describes the development of a TIGGE forecast based dynamical-statistical model for predicting weekly TC genesis probability during the SPO active TC seasons (November-April). A distinguishing feature of this approach is that predictors are physically relevant contemporaneous seasonal large-scale environment variables derived from a dynamical TIGGE prediction. This key point is different from a pure statistical method that depends on the lag relationship with past observation records. This study identifies potential predictors associated with weekly TC genesis probability from physical considerations. In addition, the dynamical model (here, TIGGE) provides a measure of predictor accuracy.

Based on the composite analysis, consistent with the findings in previously published literature, the MJO is selected as one of the key predictors for weekly TC genesis probability. TIGGE forecasts have reasonable capability in predicting the MJO; therefore, we use MJO forecasts from TIGGE as a predictor of weekly TC genesis.

The SPCZ variation is also well known to be associated with TC genesis in the South Pacific. The large-scale conditions affecting the variability of the western and eastern SPCZ are different, and the various SPCZ characteristics (i.e., strength, area, centroid latitude/longitude) are dominated by either seasonal or semi-annual variability. We chose to use low-level relative vorticity averaged from 10°S-20°S in each zone. Given the collocation between the large cyclonic vorticity and TC genesis areas, it is reasonable to use relative vorticity averaged in each zone instead of directly using various SPCZ characteristics. Based on our analysis, the area-averaged relative vorticity field is a good predictor for weekly TC genesis especially for regions west of the dateline.

The relationship between ENSO and TC activity is well known from many previous studies. Considering the relationship between ENSO and weekly TC genesis probabilities for each zone, we use the Nino3.4 index calculated from TIGGE forecasts as a predictor of weekly TC genesis. Based on the analysis, TC genesis increased east of the dateline in the warm ENSO phase years, and increased in the west in the cold ENSO phase years. This is consistent with previous studies. In the positive ENSO phase, the TC genesis is preferentially enhanced eastward to the South Pacific

Ocean, with the highest TC density centered on the dateline. In the negative ENSO phase, TC genesis positions have their maximum density further west of the dateline, because equatorial convection moves further westward.

8. FUTURE PLANS

8.1 Improvement of predictors

Recent studies demonstrated the advantages of the multi-model grand ensemble approach to forecasting the MJO. Matsueda and Endo (2011) indicated that ECMWF and UKMO generally display the best performances in predicting the MJO; however, they do not always show the best skills. ECMWF well-simulates the maintenance and onset of the MJO in phases 1-4, but not as well in other phases. The best-performing models vary with the phase of the MJO. Thus, it is necessary to consider all available models to better represent the current and predicted MJO. In addition, Kang and Kim (2010) showed that the dynamical and statistical-combined approaches provide a superior skill to any statistical and dynamical predictions, with a prediction length of 22-24 days. They suggested using the MJO for both dynamical and statistical models could improve the TC genesis forecasts, as it is one of the most critical predictors.

In addition to the MJO, SPCZ and ENSO that are discussed in this report, other physical and dynamical variables, such as the Genesis Potential (GP) index (Camargo et al. 2007) can also be considered.

$$GP = \left|10^5\eta\right|^{3/2}\left(\frac{RH}{50}\right)^3\left(\frac{PI}{70}\right)^3\left(1+0.1\,V_{shear}\right)^{-2}$$

The four different terms in GP index are absolute vorticity (η) at 850 hPa, relative humidity (RH) at 700 hPa, vertical wind shear (Vshear) between 850 and 200 hPa, and maximum potential intensity (PI). The potential intensity is calculated with the variables of sea surface temperature, vertical profiles of temperature and specific humidity. Therefore, the potential intensity depends on the air-sea thermodynamic disequilibrium. As the GP index empirically quantifies the effects of large-scale environment on tropical cyclogenesis, and considers both thermodynamic and dynamic factors for cyclogenesis, the use of terms in GP index would be good predictors of sub-seasonal TC genesis prediction.

8.2 TC statistical forecast model

The statistical model adopted to predict TC occurrence for each zone is a logistic regression model. The logistic regression method is suitable for making probabilistic forecast of TC occurrence because it will always forecast a probability of greater than 0 and less than 1 (Wilks 2006). The logistic regression fit to the data is

$$P(x)=\frac{e^{\beta_0+\beta_1 x_1+\beta_2 x_2+\cdot\cdot\cdot+\beta_m x_m}}{e^{\beta_0+\beta_1 x_1+\beta_2 x_2+\cdot\cdot\cdot+\beta_m x_m}+1}$$

where p represents the predicted probability of TC occurrence (predictand), m denotes the number of predictors, and $x_1, x_2, \ldots, x_m$ indicates multiple predictors. In addition, $\beta_o, \beta_1, \ldots, \beta_m$ is the regression constant and the corresponding regression coefficients, respectively, which are estimated using a least squares approach. Input dependent variables are in the form of a binary probability p that is assigned to be 0 if no TC genesis is observed during the week of interest, and 1 if TC genesis is observed during the period. We develop the model using overlapping weeks, starting on every day. We apply the statistical model separately for each regional zone, and for each forecast lead time. We will predict the probability that at least one TC forms in the next week for each zone.

8.3 Statistical modeling issues

In this study, it is critical to pre-define the region of interest for the TC forecast statistical model. The selection of these regions was based on geographical and physical consideration. The boundary at 150°E provides a natural geographical separation, with relatively few TCs crossing this longitude (Kim et al. 2015). The boundary of 180°E approximately separates regions that are known to oppositely respond to ENSO, a critical driver of TC activity. Forecasts using smaller zones, which would potentially be more useful, were tested with different longitude coverage for each zone. However, the models only prove skillful where there is a sufficiently dense number of TC formations. Thus, there is a trade-off between forecast skill and usefulness. In case of employing smaller zones, the statistical model itself is not established due to all zero predictions (TC genesis) on some days. However, we will further adapt this methodology to alternative zones in the future to pre-define the target regions.

The final goal of this project is to establish a TC forecast model in the Pacific Islands where TIGGE forecast data are directly collected. However, the TIGGE forecast only covers the latest 10 years from 2006, and only 92 TCs occurred during this period. This could be limiting the statistical model, because long training periods are necessary. In the future, we will investigate an alternative way to overcome this limitation.

8.4 Stepwise predictor screening

Even though all predictors can explain the sub-seasonal TC activity, the inclusion of many potential predictors in the multivariate regression does not necessarily guarantee better predictability. A careless combination of all predictors in the multivariate regression may lead to poor prediction (Wilks 2006). In particular, for the case of mutually correlated potential predictors and stepwise procedures for the predictor, screening is required in the logistic regression. We use the stepwise regression method (Hosmer and Lemeshow 2000) to select a best set of predictor variables from pools of potential predictors for each zone and each forecast lead time. The regression is repeated as the number of potential predictors increases, and the best set of predictors are determined by comparing the regression results at each predictor change. In the first step, we test the logistic regression with each variable from all potential predictors. From this, we select one variable as the most important predictor for the smallest p value. Next, we search for another variable in addition to the first-chosen predictor via the logistic regression model with multiple variables. Of the remaining variables, the second-most important predictor is selected in the second step using the smallest p value. This step is repeated until the threshold p value reaches 0.15 (the threshold used by Leroy and Wheeler 2008), indicating none of the remaining predictors improve the model by 15%.

It is noted that the chosen predictors are not entirely and physically independent of each other because the predictors have a substantial influence on ENSO. To verify the use of partly dependent predictors, we will examine a variance inflation factor

(VIF) for each predictor set for each region, and for each lead-time. The VIF measures the impact of multicollinearity among predictors in a regression model, where a larger VIF indicates a higher multicollinearity. A value of VIF equal to 10 is in general used as the critical value to identify multicollinearity (e.g., Davis et al. 1986; O'Brien 2007).

REFERENCE

Alessandri A., A. Borrelli, S. Gualdi, E. Scoccimarro, and S. Masina, 2011: Tropical cyclone count forecasting using a dynamical seasonal prediction system: sensitivity to improved ocean initialization. J. Climate, 24, 2963-2982.

Barry, R. G., and R. J. Chorley, 2003: Atmosphere, Weather and Climate. 8th ed. Routledge, 421 pp

Bougeault, P., et al., 2010: The THORPEX interactive grand global ensemble, Bull. Am. Meteorol. Soc., 91, 1059-1072. doi:10.1175/2010BAMS2853.1

Camargo, S. J., and A. G. Barnston, 2009: Experimental dynamical seasonal forecasts of tropical cyclone activity at IRI. Wea. Forecasting, 24, 472-491.

__________, K. A. Emanuel, and A. H. Sobel, 2007: Use of a genesis potential index to diagnose ENSO effects on tropical cyclone genesis. J. Clim., 20, 4819-4834.

Chand, S. S., J. L. McBride, K. J. Tory, M. C. Wheeler, and K. J. E. Walsh, 2013: Impact of different ENSO regimes on Southwest Pacific tropical cyclones. J. Climate, 26, 600-608.

Davis, C. E., J. E. Hyde, S. I. Bangdiwala, and J. J. Nelson, 1986: An example of dependencies among variables in a conditional logistic regression. Modern Statistical Methods in Chronic Disease Epidemiology, S. H. Moolgavkar and R. L. Prentice, Eds., Wiley, 140-147.

Diamond, H. J. A. M. Lorrey, and J. A. Renwick, 2013: A Southwest Pacific tropical cyclone climatology and linkages to the El Niño-Southern Oscillation. J. Climate, 26, 3-25.

Dowdy, A. J., L. Qi, D. Jones, H. Ramsay, R. Fawcett, and Y. Kuleshov, 2012: Tropical cyclone climatology of the South Pacific Ocean and its relationship to El Niño-Southern Oscillation. J. Climate, 25, 6108-6122.

Frank, W. M., 1987: Tropical cyclone formation. *A Global View of Tropical Cyclones,* Elsberry, R. L., Ed., Office of Naval Research, pp. 53-90.

____________, and P. E. Roundy, 2006: The role of tropical waves in tropical cyclogenesis. Mon. Wea. Rev., 134, 2397-2417.

Froude, L. S. R., 2010: TIGGE: Comparison of the Prediction of Northern Hemisphere extratropical cyclones by different ensemble prediction systems, Wea. Forecasting, 25, 819-836.

____________, 2011: TIGGE: Comparison of the Prediction of Southern Hemisphere extratropical cyclones by different ensemble prediction systems, Wea. Forecasting, 26, 388–398.

Goh, A. Z. C., and J. C. L. Chan, 2010: An improved statistical scheme for the prediction of tropical cyclones making landfall in South China. Wea. Forecasting, 25, 587–593.

Goh, A. Z. C., and J. C. L. Chan, 2012: Variations and prediction of the annual number of tropical cyclone affecting Korea and Japan. Int. J. Climatol., 32, 178–189.

Gottschalck, J., et al. 2010: A framework for assessing operational Madden–Julian Oscillation forecasts: A CLIVAR MJO working group project, Bull. Am. Meteorol. Soc., 91, 1247–1258, doi:10.1175/2010BAMS2816.1.

Gray, W. M., 1979: Hurricanes: their formation, structure and likely role in the tropical circulation. In: Shaw DB (ed) Meteorology over the tropical oceans. Roy. Meteor. Soc., London, pp. 155–218.

Hamill, T. M., 2012: Verification of TIGGE multimodel and ECMWF reforecast–calibrated probabilistic precipitation forecasts over the contiguous United States. Mon. Wea. Rev., 140, 2232–2252.

Hall, J. D., A. J. Matthews, and D. J. Karoly, 2001: The modulation of tropical cyclone activity in the Australian region by the Madden–Julian oscillation. Mon. Wea. Rev., 129, 2970–2982.

Hosmer, D. W., and S. Lemeshow, 2000: *Applied Logistic Regression*. 2^{nd} ed. Wiley, 373 pp.

Jiang, X., D. E. Waliser, M. C. Wheeler, C. Jones, M.–I. Lee, and S. D. Schubert, 2008: Assessing the skill of an all–season statistical forecast model for the Madden–Julian oscillation. Mon. Wea. Rev., 136, 1940–1956.

Jones, D., L. M. V. Carvalho, R. W. Higgins, D. E. Waliser, and J.–K. E. Schemm, 2004: A statistical forecast model of tropical intraseasonal convective anomalies. J. Clim., 17, 2078–2095.

Kang, I.–S. and H.–M. Kim, 2010: Assessment of MJO predictability for boreal winter with various statistical and dynamical models. J. Climate, 23, 2368–2378.

Kidwell, A., T. Lee, Y.–H. Jo, X.–H. Yan: 2016: Characterization of the variability of the South Pacific Convergence Zone using satellite and reanalysis wind products. J. Clim., 29, 1717–1732.

Kiladis, G. N., H. V. Storch, and H. V. Loon, 1989: Origin of the South Pacific Convergence Zone. J. Clim, 2, 1185–1195.

Kang, I.-S., H.-Mi. Kim, 2010: Assessment of MJO predictability for boreal winter with various statistical and dynamical models. J. Clim., 23, 2368-2378.

Kim, H.-M., and P. J. Webster, 2010: Extended-range seasonal hurricane forecasts for the North Atlantic with a hybrid dynamical-statistical model. Geophys. Res. Lett., 37, L21705, doi:10.1029/2010GL044792.

Kim, O.-Y., 2015: Cyclone-track based seasonal prediction for South Pacific tropical cyclone activity using APCC multi-model ensemble prediction. APCC 2015 Technical Report, APEC Climate Center.

Leroy, A., and M. C. Wheeler, 2008: Statistical prediction of weekly tropical cyclone activity in the southern Hemisphere. Mon. Wea. Rev., 136, 1083-1103.

Lin, H., G. Brunet, J. Derome, 2008: Forecast skill of the Madden-Julian Oscillation in Two Canadian Atmospheric Models, Mon. Wea. Rev., 136, 4130- 4149, doi:10.1175/2008MWR2459.1.

Lintner, B. R., J. D. Neelin, 2008: Eastern margin variability of the South Pacific Convergence Zone. Geophys. Res. Lett. 35, L16701.

Lo, F., and H. H. Hendon, 2000: Empirical extended-range prediction of the Madden-Julian oscillation. Mon. Wea. Rev., 128, 2528-2543.

Madden, R. A., and P. R. Julian, 1994: Observations of the 40-50-day tropical oscillation - A review. Mon. Wea. Rev., 122, 814-837.

Maloney, E. D., and D. L. Hartmann, 2000: Modulation of eastern North Pacific hurricanes by the Madden-Julian oscillation. J. Climate, 13, 1451-1460.

Matsueda, M., H. Endo, 2011: Verification of medium-range MJO forecasts with TIGGE. Geo. Res. Lett., 38, L11801, doi:10.1029/2011GL047480.

__________, and T. Nakazawa, 2015: Early warning products for severe weather events derived from operational medium-range ensemble forecast. Meteorol. Appl. 22, 213-222.

Matthews, A. J., 2012: A multiscale framework for the origin and variability of the South Pacific Convergence Zone. 138, 1165-1178.

Mo, K. C., 2001: Adaptive filtering and prediction of intraseasonal oscillations. Mon. Wea. Rev., 129, 802-817.

O'Brien, R. M., 2007: A caution regarding rules of thumb for variance inflation factors, Qual. Quant., 41, 673-690.

Ramsay, H. A., S. J. Camargo, and D. Kim, 2012: Cluster analysis of tropical cyclone tracks in the Southern Hemisphere. Clim. Dyn., 39, 897–917.

Seo, K. H., W. Wang, J. Gottschalck, Q. Zhang, J.-K. E. Schemm, W. R. Higgins, and A. Kumar, 2009: Evaluation of MJO forecast skill from several statistical and dynamical forecast models. J, Clim, 22, 2372–2388.

Su, X. H. Yuan, Y. Zhu, Y. Luo, and Y. Wang, 2014: Evaluation of TIGGE ensemble predictions of Northern Hemisphere summer precipitation during 2008–2012. J. Geophys. Res. Atmos., 199, 7292–7310.

Vincent E. M., M. Lengaigne, C. E. Menkes, N. C. Jourdain, P. Marchesiello, G. Madec, 2009: Interannual variability of the South Pacific Convergence Zone and implications for tropical cyclone genesis. Clim. Dyn., 36, 1881–1896.

Vitart, F., 2006: Seasonal forecasting of tropical storm frequency using a multi-model ensemble. Q. J. R. Meteor. Soc., 132, 647–666.

Waliser, D. E., C. Jones, J. K. E. Schemm, and N. E. Graham, 1999: A statistical extended-range tropical forecast model based on the slow evolution of the Madden-Julian oscillation. J. Climate, 12, 1918–1939.

Webster, P. J., and C. Hoyos, 2004: Prediction of monsoon rainfall and river discharge on 15-30-day time scales. Bull. Amer. Meteor. Soc., 85, 423–446.

Wheeler, M., and H. Hendon, 2004: An all-season real-time multivariate MJO index: Development of an index for monitoring and prediction. Mon. Wea. Rev., 132, 1917–1932.

Wilks, D. S., 2006: Statistical Methods in the Atmospheric Science. 2nd ed. Academic Press, 627 pp.

WMO, 2006: Workshop topic reports of the Sixth WMO International Workshop on Tropical Cyclones (IWTC-VI). World Meteorological Organization, WMO/TD 1353, 569 pp.

WMO, 2005: THORPEX, WMO-No. 978, 15 pp., Geneva, Switzerland.

WMO, 2014: Tropical cyclone operational plan for the South Pacific and South-East Indian Ocean. World Meteorological Organization, WMO/TD No. TCP-24.

Research Report 2016-02

Prediction of the sub-seasonal tropical cyclone genesis in the South Pacific: (I) Predictor identification

Ok-Yeon Kim

APEC Climate Center
12 Centum 7-ro, Haeundae-gu, Busan 48058, Republic of Korea
Tel: +82-51-745-3900 Fax: +82-51-745-3949

www.apcc21.org

ISBN 979-11-5698-153-4